DALTON
FULL PAPER

# Insertion of carbon dioxide into a rhodium(III)–hydride bond: a theoretical study †

**Yasuo Musashi** *[a] **and Shigeyoshi Sakaki** *[b]

[a] *Information Processing Center, Kumamoto University, Kumamoto 860, Japan*
[b] *Department of Applied Chemistry and Biochemistry, Faculty of Engineering, Kumamoto University, Kumamoto 860, Japan*

The insertion of $CO_2$ into the $Rh^{III}$–H bond of the rhodium dihydride complexes *cis*-$[RhH_2(PH_3)_3]^+$ and *cis*-$[RhH_2(PH_3)_2(H_2O)]^+$ was theoretically investigated by *ab initio* MO/MP2 and MP4SDQ methods. The transition state (TS) is product-like, in which an $\eta^1$-formate anion is almost formed. Its geometry is significantly influenced by the ligand *trans* to $CO_2$; the formate is considerably shifted from a position *trans* to hydride when the latter is *trans* to $CO_2$, but only slightly when either $PH_3$ or $H_2O$ is *trans* to $CO_2$. The activation barrier ($E_a$) and the reaction energy ($\Delta E$) were calculated to be 53.8 and −3.3 kcal mol$^{-1}$, respectively, when the hydride ligand is *trans* to $CO_2$, 41.7 and −8.0 kcal mol$^{-1}$ when $PH_3$ is *trans* to $CO_2$ and 24.0 and −27.0 kcal mol$^{-1}$ when $H_2O$ is *trans* to $CO_2$, where MP4SDQ values are given and a negative $\Delta E$ value indicates that the reaction is exothermic. These results are clearly understood in terms of the *trans* influence of H (hydride), $PH_3$ and $H_2O$.

Catalytic synthesis of formic acid from $CO_2$ and $H_2$ [equation (1)] is considered an attractive $CO_2$ fixation reaction.[1–5] This

$$CO_2 + H_2 \xrightarrow{[Rh(nbd)(PMe_2Ph)_3]BF_4} HCO_2H \qquad (1)$$

reaction involves insertion of $CO_2$ into a metal–hydride bond as a key step. In this regard, detailed knowledge on this insertion step is necessary further to develop this catalytic reaction. Previously, we theoretically investigated the insertion of $CO_2$ into a $Rh^{III}$–H bond [equation (2)] with *ab initio* MO/MP4,

$$cis\text{-}[RhH_2(PH_3)_3]^+ + CO_2 \longrightarrow [RhH(O_2CH)(PH_3)_3]^+ \qquad (2)$$

single double excitation-configuration interaction (SD-CI) and coupled cluster with double excitations calculation (CCD) methods,[6] since a rhodium(III) dihydride complex was proposed as an active species in reaction (1).[1] One of the important results was that the activation barrier ($E_a$) was calculated to be significantly high (52.3 kcal mol$^{-1}$ at the MP4SDQ level) and seems too high to perform easily the fixation of $CO_2$. Thus, we need to investigate the insertion of $CO_2$ into the $Rh^{III}$–H bond in more detail, and to find the conditions that facilitate it.

In the present work the insertion of $CO_2$ into the $Rh^{III}$–H bond of *cis*-$[RhH_2(PH_3)_3]^+$ and *cis*-$[RhH_2(PH_3)_2(H_2O)]^+$ was theoretically investigated with *ab initio* MO/MP2 and MP4SDQ methods, where three types of insertion reaction (A–C) were examined, as shown in Scheme 1; the hydride ligand is *trans* to $CO_2$ in insertion A, $PH_3$ in B, and $H_2O$ in C. Our purposes here are to estimate reliably an activation barrier ($E_a$) and a reaction energy ($\Delta E$), to present a clear understanding of the $CO_2$-insertion reaction, to shed some light on the active species of the rhodium-catalysed $CO_2$-fixation reaction, and to propose a good rhodium complex for the insertion.

## Computations

In our previous work[6] geometries were optimized at the Hartree–Fock (HF) level and the basis sets used were not sufficiently good. In the present work, the geometries of the reactants, precursor complex, transition state (TS) and product were optimized at the MP2 level with better basis sets, and then MP4SDQ calculations were carried out with those optimized geometries, where core orbitals were excluded from the active space. All the calculations were carried out with the GAUSSIAN 94 program.[7]

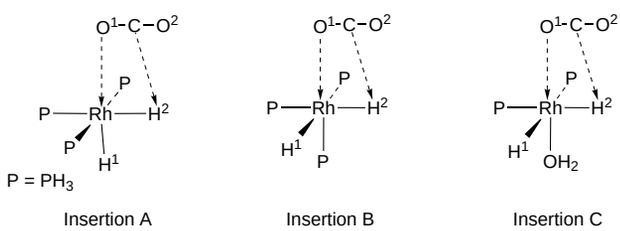


**Scheme 1**

Two kinds of basis set system were used in these calculations. In the small basis set (BS I) core electrons of Rh (up to 3d) were replaced with effective core potentials (ECPs) of Hay and Wadt,[8] and its valence electrons were represented with a (311/311/211) set. MIDI-4[9] Sets were used for P, C and O, where a d-polarization function was added to all these atoms. The (4s)/[2s] set[10] was used for H, where a p-polarization function was added on the active hydrogen atom (a hydride) and the H atom of formate. In the large basis set system (BS II) a more flexible contraction (541/541/211) was employed for Rh,[11] where the same ECPs as those in BS I were used. (9s 5p 1d)/[3s 2p 1d] Sets[10] augmented with a p-diffuse function were used for C and O, and a (5s 1p)/[3s 1p] set[12] augmented with an s-diffuse function was employed for the active H atom. For the other atoms the same basis sets as those in BS I were used. The BS I system was employed for geometry optimization and the BS II system for calculation of energy change. In evaluating binding energy and $E_a$ values, the basis-set superposition error (BSSE) was corrected at the MP4SDQ level with the Boys method.[13]

## Results and Discussion

### Geometries of precursor complex, transition state (TS) and product

Geometry changes of three insertion reactions are shown in Fig. 1. In the precursor complex the Rh–$O^1$ and C–$H^2$ distances are very long, and both $CO_2$ and $RhH_2(PH_3)_2L$ (L = $PH_3$ or

† *Non-SI units employed*: cal = 4.184 J, eV ≈ 1.60 × 10$^{-19}$ J.

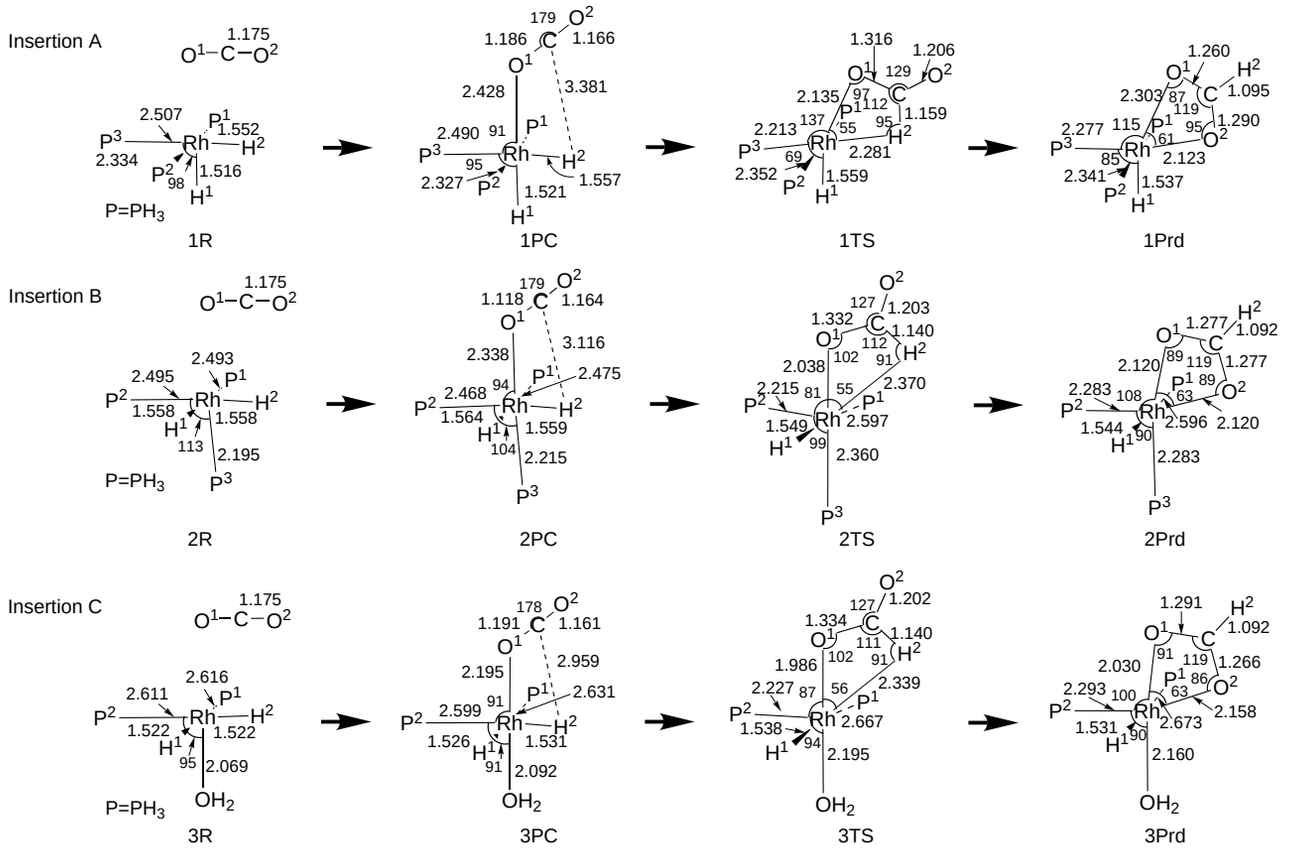


**Fig. 1** Geometry changes in the insertion of $CO_2$ into the $Rh^{III}$–H bond of *cis*-$[RhH_2(PH_3)_3]^+$ (insertions A and B, Scheme 1) and *cis*-$[RhH_2(PH_3)_2(H_2O)]^+$ (insertion C). Bond distances in Å and angles in °

$H_2O$) moieties distort little, as is commonly observed in many insertions of $CO_2$ into metal–hydride and –alkyl bonds.[6,14] These geometrical features suggest that $CO_2$ cannot form a strong co-ordinate bond with $Rh^{III}$, as expected. Although the above-mentioned features are commonly observed, several differences are found among these insertion reactions. For instance, the Rh–$O^1$ and C–$H^2$ distances become shorter in the order insertion A > B > C. Although the Rh–$H^1$ bond length of **1PC** is almost the same as that of **1R**, the Rh–$P^3$ bond of **2PC** is 0.02 Å longer than that of **2R**, and the Rh–$OH_2$ bond of **3PC** is 0.023 Å longer than that of **3R**. These geometrical changes indicate that the co-ordination of $CO_2$ is influenced by the ligand at the *trans* position of $CO_2$, and at the same time the Rh–$PH_3$ and Rh–$OH_2$ co-ordinate bonds positioned *trans* to $CO_2$ are also influenced by the co-ordination of $CO_2$ whereas the latter co-ordination is weak.

In the TS of the three insertion reactions the Rh–$O^1$ distance is shorter than that in the product, the C–$H^2$ distance is only 0.1 Å longer than that in the product, and the Rh–$H^2$ distance is about 2.3 Å, being much longer than that in the reactant. These geometrical features indicate that this TS is product-like and an $\eta^1$-formate anion is almost formed at the TS. It should be noted here that the TS geometry exhibits interesting differences among the three insertion reactions. In the TS of insertion A (**1TS**) the $O^1$ atom significantly shifts from the *z* axis, while in the TSs (**2TS** and **3TS**) of insertions B and C the $O^1$ atom shifts slightly. The Rh–$H^1$ distance lengthens by only 0.035 Å in **1TS**, while the Rh–$P^3$ and Rh–$OH_2$ distances lengthen by 0.15 and 0.1 Å in **2TS** and **3TS**, respectively. These differences in TS geometry are interpreted in terms of *trans* influence, as will be discussed below in detail.

In the product the formate anion co-ordinates to Rh in a bidentate way, because the rhodium(III) ion tends to form a six-co-ordinate complex due to its $d^6$ electron configuration. This would be a reason that the Rh–$O^1$ distance in the TS is slightly shorter than that in the product, as follows: since the $\eta^1$-formate has only one Rh–O interaction but the $\eta^2$-formate has two, the one interaction of the $\eta^1$-formate would be stronger than that in the $\eta^2$-formate, which leads to the slightly shorter Rh–$O^1$ distance in the TS than that in the product (remember the $\eta^1$-formate is almost formed at the TS, while the product involves the $\eta^2$-formate). The geometries are also different among these insertion reactions like their TS geometries. For instance, the $P^3$–Rh–$O^1$ angle increases in the order **3Prd** < **2Prd** < **1Prd**; *i.e.* the $O^1$ atom considerably shifts from the *z* axis in the product (**1Prd**) of insertion A, but slightly shifts in the product (**3Prd**) of insertion C. Again, these geometrical features would be related to the *trans* influence.

Here, we must mention how the geometry reaches the product from the TS. The best way to investigate this geometry change is to carry out an intrinsic reaction coordinate (IRC) calculation.[15] However, IRC calculations of transition-metal systems at the MP2 level are very time-consuming. Therefore, we investigated plausible geometry changes,[14a] as follows: one is the opening of the Rh–$O^1$–C angle (path 1) and the other is rotation of the $\eta^1$-formate moiety around the C–$O^1$ bond (path 2). In path 1 we optimized the geometry at various Rh–$O^1$–C angles. As shown in Fig. 2, the energy rapidly lowers upon opening the Rh–$O^1$–C angle and the system reaches the local minimum (**1La**) at Rh–$O^1$–C *ca.* 130°. After **1La** the system smoothly changes to the final product through **1TSa** which is at Rh–$O^1$–C 163°.‡ The TS is 5 kcal $mol^{-1}$ above **1La** (MP2/BS I calculation). In path 2 the dihedral angle ($\phi$) between the Rh$O^1$C and $O^2CH^2$ planes was taken as a reaction coordinate and the geometry optimized at various $\phi$ angles. In this case a local minimum (**1Lb**) is observed at $\phi = 5°$, as shown in Fig. 3. Although the geometry of **1Lb** differs much from that of **1TS**, the opening of the $P^3$–Rh–$O^1$ angle smoothly connects these two structures without a barrier (Fig. 3). The system reaches

‡ This TS was not fully optimized but roughly determined by taking the Rh–$O^1$–C angle as a reaction coordinate.

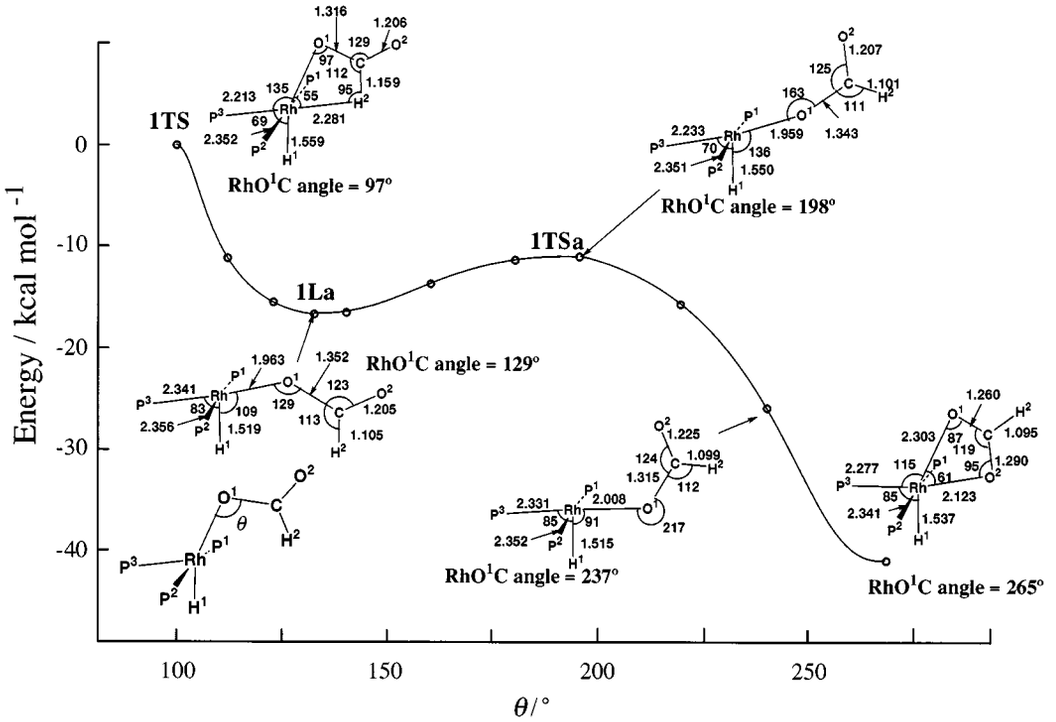


**Fig. 2** Energy and geometry changes (MP2/BS I calculation, energy relative to **1TS**) after **1TS** upon opening of the Rh–O$^1$–C angle θ. Bond distances in Å and angles in °

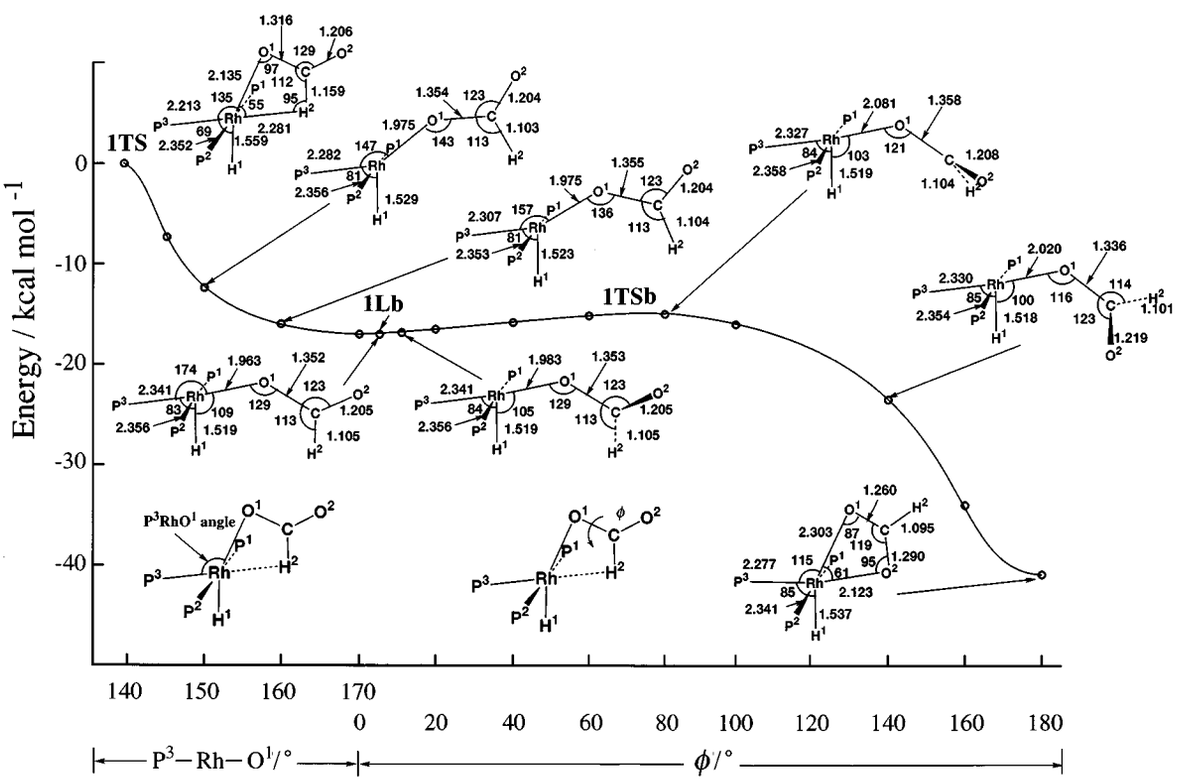


**Fig. 3** Energy and geometry changes (MP2/BS I calculation, energy relative to **1TS**) after **1TS** upon rotation of the formate moiety around the C–O$^1$ bond; φ = dihedral angle between the RhO$^1$C and O$^2$CH$^2$ planes

the **1TSb**§ at φ = 80°. After this TS the system gets to the final product $[RhH(\eta^2\text{-}O_2CH)(PH_3)_3]^+$. The TS is only 2 kcal mol$^{-1}$ above **1Lb** (MP2/BS I calculation). Thus, the geometry change through path 2 occurs more easily than that through path 1, and **1TS** is the real transition state of the insertion.

§ This TS was not fully optimized but roughly determined by taking the dihedral angle (φ) between the RhO$^1$C and O$^2$CH$^2$ planes as a reaction coordinate.

In conclusion, the system smoothly reaches the final product by rotation of the formate moiety around the C–O$^1$ bond.

### Binding energy (BE), activation barrier ($E_a$) and reaction energy ($\Delta E$) in three insertion reactions

The binding energy (BE) is defined as a stabilization energy of the precursor complex (PC) relative to the sum of reactants {BE = $E_t[RhH_2L(PH_3)_2^+] + E_t(CO_2) - E_t(PC)$}, the activation barrier ($E_a$) is the energy difference between PC and TS [$E_a$ =

**Table 1** Binding energy of the precursor complex (BE),[a] activation energy ($E_a$)[b] and reaction energy ($\Delta E$)[c] of insertions A, B and C[d] (all values in kcal mol$^{-1}$)

| Insertion | BE | $E_a$ | $\Delta E$ |
|---|---|---|---|
| (*a*) MP4SDQ/BS II[e] | | | |
| A | 12.4 (6.3) | 53.8 (59.9) | −3.3 |
| B | 14.2 (7.4) | 41.7 (51.5) | −8.0 |
| C | 19.1 (12.8) | 24.0 (30.1) | −27.0 |
| (*b*) MP2/BS I | | | |
| A | 13.2 | 55.2 | −1.8 |
| B | 14.2 | 45.2 | −4.4 |
| C | 19.2 | 24.5 | −26.2 |

[a] The energy difference between the precursor complex and the sum of the reactants, BE = $E_t[RhH_2(PH_3)_2L^+] + E_t(H_2O) - E_t[RhH_2(PH_3)_2L(H_2O)^+]$. A positive value represents the stabilization of the precursor complex relative to the reactants. [b] The energy difference between the precursor complex and the TS, $E_a = E_t(TS) - E_t(PC)$. [c] The energy difference between the product and the sum of the reactants, $\Delta E = E_t(Prd) - E_t[RhH_2(PH_3)_2L^+] - E_t(CO_2)$. A negative value indicates that the reaction is exothermic. [d] See Scheme 1 for insertions A, B and C. [e] Values after correction[13] for the basis set superposition error are given in parentheses.

$E_t(TS) - E_t(PC)$], and the reaction energy ($\Delta E$) is the energy difference between the product and the sum of reactants {$\Delta E = E_t(Prd) - E_t[RhH_2L(PH_3)_2^+] - E_t(CO_2)$}. A positive BE value means that the PC is more stable than the sum of reactants, and a negative $\Delta E$ value that the reaction is exothermic. Values of BE, $E_a$ and $\Delta E$ of the three insertion reactions were calculated with the MP4SDQ/BS II method and are listed in Table 1. The $E_a$ value of insertion A is very large, indicating that insertion A is very difficult. On the other hand, BE, $E_a$ and $\Delta E$ of insertions B and C are much different from those of A. The BE value increases in the order insertion A < B < C, $E_a$ decreases very much in the order A > B > C, and the exothermicity increases in the order A < B < C. It should be noted that insertion B proceeds with $E_a$ of 42 kcal mol$^{-1}$, 12 kcal mol$^{-1}$ lower than that of A, and insertion C takes place with a much lower $E_a$ of 24 kcal mol$^{-1}$. In other words insertion reactions B and C occur more easily than A, and in particular C proceeds the most easily.

The BSSE correction[13] decreases the BE value by 6–7 kcal mol$^{-1}$ and increases the $E_a$ value by 6–10 kcal mol$^{-1}$, as shown in Table 1. However, the insertion of $CO_2$ becomes more easy in the order A < B < C even after BSSE correction, indicating that the same discussion can be presented after BSSE correction. Results of the MP2/BS I calculations are also given in Table 1. The BE, $E_a$ and $\Delta E$ values are not very much different between the MP2/BS I and MP4SDQ/BS II calculations. This means that the MP2/BS I optimization seems reasonable.

It is of considerable importance to clarify the reason why the significantly large $E_a$ difference exists among the three insertion reactions. Such knowledge would be useful to find a new efficient catalyst for the fixation of $CO_2$. The reason should be found in the bonding nature of the TS. As discussed above, the formate anion is almost formed at a *trans* position of the hydride in the TS of insertion A. This structure would be very unstable, because the hydride ligand exhibits strong *trans* influence. In the TS of insertion B the formate is *trans* to $PH_3$ and that of C, it is *trans* to $H_2O$. These structures would be more stable because $PH_3$ and $H_2O$ exhibit weak *trans* influence. Thus, a detailed investigation of the *trans* influence is necessary to understand the reactivity of $CO_2$ in this insertion.

### *trans* Influence of H (hydride), $PH_3$ and $H_2O$

Although we believe that the *trans* influence becomes stronger in the order $H_2O < PH_3 < H$ (hydride), we investigated it in detail. To clarify the difference in *trans* influence, [$RhH_2(PH_3)_3(H_2O)$]$^+$ **4A** and **4B** and [$RhH_2(PH_3)_2(H_2O)_2$]$^+$ **4C** were investigated, where a hydride ligand is *trans* to $H_2O$ in **4A**, $PH_3$ is *trans* to $H_2O$ in **4B**, and $H_2O$ *trans* to the other $H_2O$ in **4C**, as shown in Fig. 4. These compounds were selected because the difference in *trans* influence would be clearly shown in such a weak co-ordinate bond as the $Rh^{III}$–$H_2O$ bond. Apparently, the $Rh^{III}$–$H_2O$ bond becomes longer in the order **4C** < **4B** < **4A**, and the $H_2O$-binding energy decreases in the order **4C** > **4B** > **4A** (Fig. 4), where the binding energy is defined as an energy difference between [$RhH_2(PH_3)_2L(H_2O)$]$^+$ (L = $PH_3$ or $H_2O$) and the sum of [$RhH_2(PH_3)_2L$]$^+$ and $H_2O$, BE = $E_t[RhH_2(PH_3)_2L^+] + E_t(H_2O) - E_t[RhH_2(PH_3)_2L(H_2O)^+]$. These results clearly show that the *trans* influence increases in the order $H_2O < PH_3 < H$ (hydride), as we expected. Although the $E_a$ difference is larger than the difference in the $H_2O$-binding energy, it is reasonably concluded that the *trans* influence is one of the important factors in determining the activation barrier to insertion of $CO_2$.

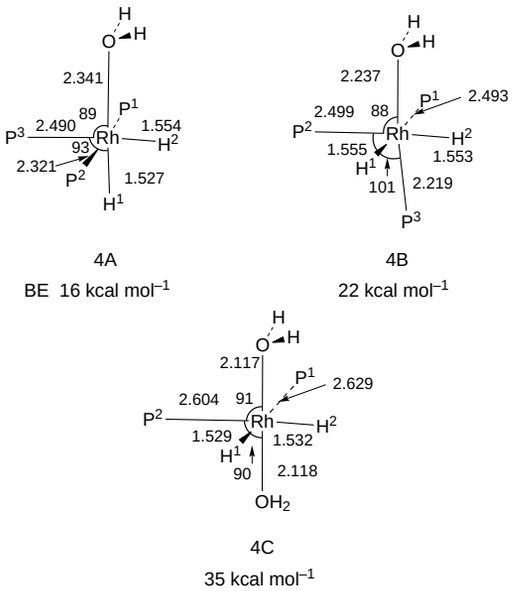


**Fig. 4** Optimized geometries of [$RhH_2(PH_3)_3(H_2O)$]$^+$ and [$RhH_2(PH_3)_2(H_2O)_2$]$^+$ from MP4SDQ/BS II calculations. The binding energy of $H_2O$, BE = $E_t[RhH_2(PH_3)_2L^+] + E_t(H_2O) - E_t[RhH_2(PH_3)_2L(H_2O)^+]$ (L = $PH_3$ or $H_2O$)

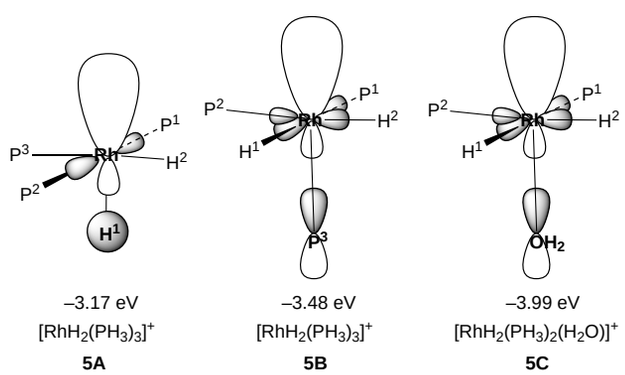


**Scheme 2** The LUMO of [$RhH_2(PH_3)_3$]$^+$ and [$RhH_2(PH_3)_2(H_2O)$]$^+$

The *trans* influence is related to the LUMO of [$RhH_2(PH_3)_3$]$^+$ and [$RhH_2(PH_3)_2(H_2O)$]$^+$, since both co-ordinate bonds of $H_2O$ and formate anion are formed through σ donation to $Rh^{III}$. The LUMO energy level of [$RhH_2(PH_3)_3$]$^+$ **5A** and **5B** and [$RhH_2(PH_3)_2(H_2O)$]$^+$ **5C** was calculated, as shown in Scheme 2, where $H_2O$ was removed from **4A**–**4C**. The LUMO mainly consists of the rhodium $d_{z^2}$ orbital which undergoes an antibonding mixing with the hydride 1s orbital in **5A**, the $PH_3$ lone-pair orbital in **5B** and the $H_2O$ lone-pair orbital in **5C**. Since the hydride ligand can form a strong bond with the rhodium $4d_{z^2}$

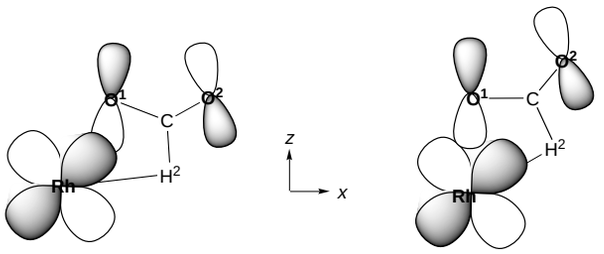


$z$—Rh—$O^1$ angle = 26° ≈ 0°

Large $d_{xz}$ – O lone pair repulsion Small $d_{xz}$ – O lone pair repulsion

No $d_\pi$ – H 1s repulsion Large $d_\pi$ – H 1s repulsion

**Scheme 3**

orbital in the occupied space, the latter orbital undergoes substantial antibonding mixing with the hydride 1s orbital in the LUMO, and therefore the LUMO of **5A** rises in energy. On the other hand, the co-ordinate bond of $H_2O$ with Rh is weak, and therefore the rhodium $4d_{z^2}$ orbital undergoes less antibonding mixing with the $H_2O$ lone-pair orbital. The co-ordination of $PH_3$ is intermediate in strength between those of hydride and $H_2O$. As a result the LUMO rises in energy in the order **5C** (−3.99 eV) < **5B** (−3.48 eV) < **5A** (−3.17 eV). Thus, the co-ordination of $H_2O$ becomes stronger in the order **5A** < **5B** < **5C**. Consistent with this result, the natural bond orbital (NBO) population [16] of $H_2O$ decreases upon co-ordination by −0.176 e in **4A**, −0.228 e in **4B** and −0.266 e in **4C**, indicating that the donating interaction of $H_2O$ becomes weaker in the order **4C** > **4B** > **4A**. From these results, it is reasonably concluded that the *trans* influence strengthens in the order $H_2O < PH_3 <$ hydride because these ligands suppress the σ donation from the other ligand to Rh in this order.

### Geometry differences of the TS and product among the three reaction systems

The differences in TS geometry are easily understood in terms of the *trans* influence and the exchange repulsion between the formate and the doubly occupied rhodium $d_{xz}$ orbital. In **1TS** the $O^1$ atom is *trans* to a hydride. Owing to the strong *trans* influence of hydride, the $O^1$ position shifts from the $z$ axis. This geometry leads to the small overlap between the rhodium $d_{z^2}$ orbital and the formate $O^1$ lone-pair orbital, and gives rise to the exchange repulsion between the rhodium $d_{xz}$ orbital and the formate $O^1$ lone-pair orbital, as shown in Scheme 3. Therefore, the Rh–$O^1$ bond becomes weak, which is reflected in the long Rh–$O^1$ bond. In this geometry, however, the $H^2$ atom does not cause the exchange repulsion with the rhodium $d_{xz}$ orbital. In **2TS** and **3TS** of insertions B and C the $O^1$ atom slightly shifts from the $z$ axis, due to the weak *trans* influence of $PH_3$ and $H_2O$. As a result, the $O^1$ lone-pair orbital can strongly interact with the rhodium $d_{z^2}$ orbital, leading to the stronger Rh–$O^1$ bond in **2TS** and **3TS** than in **1TS**. Actually, the Rh–$O^1$ distance of **2TS** and **3TS** is much shorter than that in **1TS**; *i.e.* 2.135 Å in **1TS**, 2.038 Å in **2TS** and 1.986 Å in **3TS**. In **2TS** and **3TS**, however, the $H^2$ atom must adopt an unfavorable position overlapping with the rhodium $d_{xz}$ orbital, resulting in the exchange repulsion with this orbital (Scheme 3). Consequently, the Rh–$H^2$ distance is considerably long in **2TS** and **3TS**.

In the TS for insertion of $CO_2$ the $O^1$ NBO population [16] decreases in the order **1TS** (8.69 e) > **2TS** (8.59 e) > **3TS** (8.55 e). This result demonstrates that the $O^1$ atom of formate donates its lone-pair electrons to Rh the most in **3TS**, less in **2TS** and the least in **1TS**, and the $\eta^1$-formate interaction with Rh becomes stronger in the order **1TS** < **2TS** < **3TS**. Thus, the barrier decreases in the order insertion A > B > C.

The geometry differences in the products are explained similarly. In **1Prd** the $O^1$ atom avoids being *trans* to hydride because of the strong *trans* influence of the latter. This geometry leads to the small overlap between the $O^1$ lone-pair and rhodium $d_{z^2}$ orbitals, and gives rise to the large exchange repulsion between the $O^1$ lone-pair and rhodium $d_{xz}$ orbitals. Thus, the Rh–$O^1$ bond is very long (2.303 Å). In **3Prd** the $O^1$ atom slightly shifts from the $z$ axis, because of the weak *trans* influence of $H_2O$. Since the $O^1$ lone-pair orbital overlaps well with the rhodium $d_{z^2}$ orbital and does not cause exchange repulsion with the rhodium $d_{xz}$ orbital, the Rh–$O^1$ bond is shorter than that in **1Prd**. However, the $O^2$ atom must shift from the $x$ axis and causes exchange repulsion with the rhodium $d_{xz}$ orbital. Thus, the Rh–$O^2$ distance of **3Prd** is the longest (2.158 Å) in the three products. The **2Prd** geometry is intermediate between those of **1Prd** and **3Prd**. The $O^1$ NBO population decreases in the order **1Prd** (8.60 e) > **2Prd** (8.54 e) > **3Prd** (8.52 e), which is consistent with the Rh–$O^1$ bond becoming stronger in the order **1Prd** < **2Prd** < **3Prd**.

In conclusion, the *trans* influence and the exchange repulsion between formate and the rhodium $d_{xz}$ orbital are important factors in determining the geometries of the TS and product.

### Changes in bonding nature upon insertion of $CO_2$

As shown in Fig. 5, the NBO population [16] of $CO_2$ considerably increases as the insertion proceeds, while those of Rh and $PH_3$ decrease very much. These population changes suggest that charge transfer to $CO_2$ from Rh is necessary to change $CO_2$ into the formate anion. Interestingly, the $CO_2$ population at the TS is almost the same as that of the product, clearly indicating that the formate anion is almost formed at the TS. This is consistent with the TS geometry in which the $CO_2$ + H geometry resembles well that of the $\eta^1$-formate anion. The $H^2$ NBO population is expected to decrease at the TS, since the hydride ligand changes into the H atom of formate and charge transfer occurs significantly from $[RhH_2(PH_3)_2L]^+$ to $CO_2$. However, the $H^1$ NBO population slightly increases at the TS and then slightly decreases at the product. This population change suggests that not only the charge transfer from $H^2$ to $CO_2$ but also that from Rh to $H^2$ occurs to facilitate the charge transfer from $H^2$ to $CO_2$, as shown in Scheme 4. The NBO population of $PH_3$ also decreases in the reaction, indicating that Rh is supplied electrons by $PH_3$. In other words, Rh and $PH_3$ play the role of electron pools. Since the H atom of formate is covalently bound to the C atom and since its NBO population is little different from that of the hydride (see Fig. 3), the hydride ligand is considered to be covalently bound to Rh. From these population changes, a coherent picture might emerge, as follows: (1) the insertion of $CO_2$ needs charge transfer to $CO_2$ from $[RhH_2(PH_3)_2L]^+$, (2) the hydride ($H^2$) ligand which is covalently bound to Rh does not have enough electrons to cause the charge transfer to $CO_2$, and (3) Rh must supply electrons to $H^2$, which is assisted by the charge transfer from $PH_3$ to Rh.

### Active species of rhodium-catalysed formate synthesis

In the catalytic reaction the vacant site of **1R**, **2R** and **3R** would be occupied by a solvent molecule such as tetrahydrofuran (thf) or water (remember that thf involving a few % of water was used as a solvent in the catalytic reaction).[1] Thus, we consider that the insertion of $CO_2$ starts from **4A**, **4B** and **4C** in which the vacant site of **1R**, **2R** and **3R** is occupied by $H_2O$. As shown in Fig. 6, **4A** is the most stable, **4B** the next, and **4C** the least stable.¶ The relative stabilities of **4A** and **4B** are attributed to the *trans* influence. In **4A**, $H_2O$ is *trans* to a hydride. In **4B** two hydride ligands are *trans* to $PH_3$. This geometry is less favorable

¶ The stability of species **4C** was compared with that of **4A** by considering the equation **4A** + $H_2O$ ⟹ **4C** + $PH_3$. In other words, the energy of **4A** + $H_2O$ was taken as a standard (energy zero), and that **4C** + $PH_3$ was compared with that of **4A** + $H_2O$.

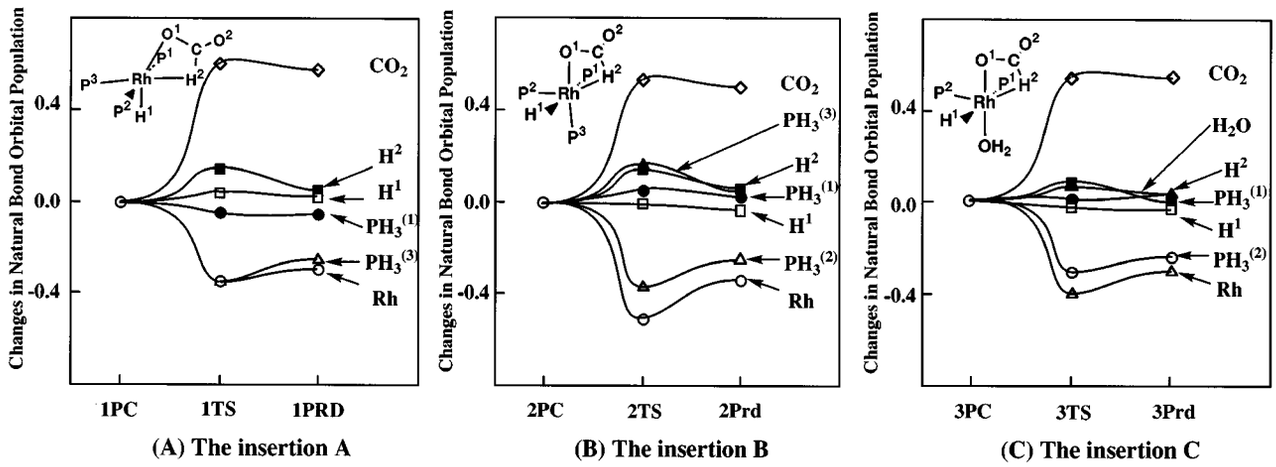


**Fig. 5** Natural bond orbital population changes upon insertion of $CO_2$ into the $Rh^{III}$–H bond of *cis*-$[RhH_2(PH_3)_3]^+$ (insertions A and B) and *cis*-$[RhH_2(PH_3)_2(H_2O)]^+$ (insertion C). A positive value represents an increase in population relative to the precursor complex and *vice versa*

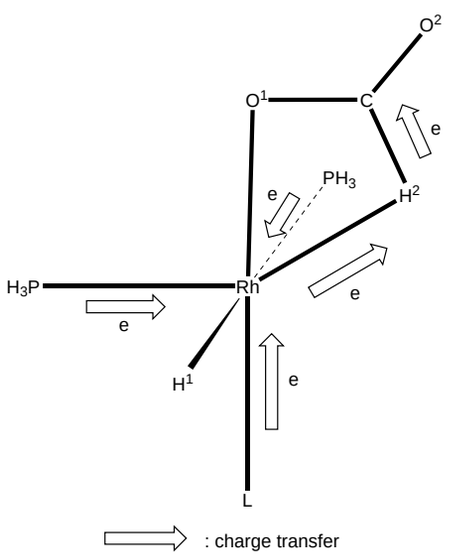


**Scheme 4**

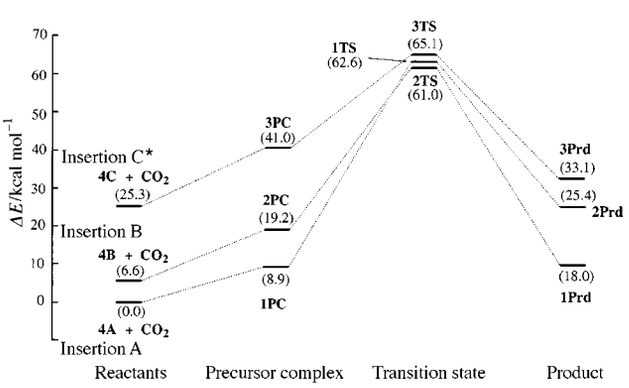


**Fig. 6** Energy changes in insertions A, B and C obtained by MP4SDQ/BS II calculations. Numbers are the energies (kcal $mol^{-1}$) relative to species **4A** + $CO_2$. * Energy of **4C** + $PH_3$ relative to **4A** + $H_2O$

than **4A**. The lowest stability of **4C** results from the $H_2O$ co-ordinate bond; **4C** has two $H_2O$ and two $PH_3$ ligands, while **4A** and **4B** have one $H_2O$ and three $PH_3$ ligands. Since the $H_2O$ co-ordinate bond is weaker than that of $PH_3$, **4C** is the least stable.

Although species **4A** is the most stable, the insertion A starting from **4A** is the most difficult: an energy destabilization of 9 kcal $mol^{-1}$ occurs to yield **1PC**, and then the much higher activation barrier of 54 kcal $mol^{-1}$ is necessary for the insertion. In insertion C, on the other hand, an energy destabilization of 16 kcal $mol^{-1}$ is necessary to yield **3PC**, but the insertion easily proceeds with the moderate activation barrier of 24 kcal $mol^{-1}$. Since **4C** is 25 kcal $mol^{-1}$ less stable than **4A**, the concentration of **4C** is considerably low. However, this concentration would increase even under milder conditions than those of insertion A, since the barrier to the latter is much higher than the energy difference between **4A** and **4C**. This means that although **4C** is much less stable than **4A** the insertion C occurs more easily than A. In insertion B, an energy destabilization of 6.6 kcal $mol^{-1}$ is necessary to reach **2PC**, and then the activation barrier of 41.8 kcal $mol^{-1}$ is required for the $CO_2$ insertion. This situation is better than that in insertion A, but much worse than that in C. Thus, it should reasonably be concluded that **4C** is the most favorable active species in the Rh-catalysed fixation of $CO_2$.

If $PH_3$ dissociates from $Rh^{III}$, a solvent (solv) such as thf and water can co-ordinate to form $[RhH_2(PH_3)_2(solv)]^+$. The present calculations clearly indicate that the insertion of $CO_2$ occurs much more easily in this species than in $[RhH_2(PH_3)_3]^+$. In fact, $[RhH_2(PH_3)_2(solv)]^+$ was experimentally proposed as an intermediate.[1] To yield this species, an excess of phosphine should not be added to the reaction solution and a solvent facilitating phosphine dissociation must be used in this kind of $CO_2$-fixation reaction. Consistent with this discussion, it was experimentally reported that an excess of phosphine suppressed formate formation.[1]

## Conclusion and Prediction

The insertion of $CO_2$ into the $Rh^{III}$–H bond of $[RhH_2(PH_3)_3]^+$ and $[RhH_2(PH_3)_2(H_2O)]^+$ was theoretically investigated with *ab initio* MO/MP2 and MP4SDQ methods. One of the important results is that the insertion requires a much higher activation barrier of *ca.* 54 kcal $mol^{-1}$ when the hydride ligand is *trans* to $CO_2$ (insertion A). If the ligand *trans* to $CO_2$ is $PH_3$ (insertion B) the activation barrier is lowered by *ca.* 10 kcal $mol^{-1}$. When $H_2O$ is *trans* to $CO_2$ (insertion C) the insertion proceeds much more easily with an activation energy of 24 kcal $mol^{-1}$. Thus, *cis*-$[RhH_2(PH_3)_2(H_2O)_2]^+$ **4C** is considered to be a good active species in this fixation of $CO_2$, as suggested experimentally.[1] The differences among the three insertion reactions are interpreted in terms of the *trans* influence of hydride, $PH_3$ and $H_2O$ ligands and the exchange repulsion between the $O^1$ lone pair of formate and the rhodium $d_{xz}$ orbital. The *trans* influence is analysed in detail, based on the co-ordination of $H_2O$ to $[RhH_2(PH_3)_2L]^+$ (L = $PH_3$ or $H_2O$), the charge transfer from $H_2O$ to Rh, and LUMO energy level of $[RhH_2(PH_3)_2L]^+$.

The insertion of $CO_2$ into the $Rh^{III}$–H bond is characterized as an electrophilic attack of $CO_2$ on $[RhH_2(PH_3)_2L]^+$, in which the covalent $Rh^{III}$–H bond is lost and an ionic rhodium(III)–

formate bond is formed, and significant charge transfer occurs from $[RhH_2(PH_3)_2L]^+$ to $CO_2$.

From the above discussion we can propose ways of facilitating insertion of $CO_2$ into the $Rh^{III}$–H bond. One is to use a tripodal phosphine ligand, in which the position *trans* to $CO_2$ is always occupied by phosphine. Thus, insertion B which is more favorable than A occurs in this case. The other is to use a solvent facilitating phosphine dissociation. In this case, $[RhH_2(PH_3)_2(solv)]^+$ would be formed and insertion C can occur. This insertion is much more favorable than A and B. Of course an excess of phosphine is unfavorable, since it suppresses the formation of $[RhH_2(PH_3)_2(solv)]^+$.[1]

## Acknowledgements

All the calculations were carried out with the HP Exemplar SPP1000/XA8 scalable parallel processor at the Information Processing Center of Kumamoto University and the IBM SP2 computer of the Institute for Molecular Science (Okazaki, Japan). This work was financially supported in part by a Grant-in-Aid for Scientific Research on Priority Areas (Inter Element Linkage) from the Ministry of Education, Culture and Science (No. 09239105).

## References

1 J.-C. Tsai and K. M. Nicholas, *J. Am. Chem. Soc.*, 1992, **114**, 5117.
2 D. J. Darensbourg, G. Grötsch, P. Wiegreffe and A. L. Rheingold, *Inorg. Chem.*, 1987, **26**, 3827.
3 W. Kaska, S. Nemeh, A. Shirazi and S. Potunik, *Organometallics*, 1988, **7**, 13.
4 (*a*) T. Burgemeiser, F. Kastner and W. Leitner, *Angew. Chem.*, *Int. Ed. Engl.*, 1993, **32**, 739; (*b*) F. Hutschka, A. Dedieu and W. Leitner, *Angew. Chem.*, *Int. Ed. Engl.*, 1995, **34**, 1742; (*c*) F. Hutschka, A. Dedieu, M. Eichberger, R. Fornika and W. Leitner, *J. Am. Chem. Soc.*, 1997, **119**, 4432.
5 P. G. Jessop, T. Ikariya and R. Noyori, *J. Am. Chem. Soc.*, 1996, **118**, 344.
6 S. Sakaki and Y. Musashi, *Int. J. Quantum Chem.*, 1996, **57**, 481.
7 M. J. Frisch, G. W. Trucks, H. B. Schlegel, P. M. W. Gill, B. G. Johnson, M. A. Robb, J. R. Cheeseman, T. A. Keith, G. A. Petersson, J. A. Montgomery, K. Raghavachari, M. A. Al-Laham, V. G. Zakrzewski, J. V. Ortiz, J. B. Foresman, J. Cioslowski, B. B. Stefanov, A. Nanayakkara, M. Challacombe, C. Y. Peng, P. Y. Ayala, W. Chen, M. W. Wong, J. L. Andres, E. S. Replogle, R. Gomperts, R. L. Martin, D. J. Fox, J. S. Binkley, D. J. Defrees, J. Baker, J. P. Stewart, M. Head-Gordon, C. Gonzalez and J. A. Pople, GAUSSIAN 94, Gaussian Inc., Pittsburg, PA, 1995.
8 P. J. Hay and W. R. Wadt, *J. Chem. Phys.*, 1985, **82**, 270.
9 S. Huzinaga, J. Andzelm, M. Klobukowski, E. Radzio-Andzelm, Y. Sakai and H. Tatewaki, *Gaussian Basis Sets for Molecular Calculations*, Elsevier, Amsterdam, 1984.
10 T. H. Dunning and P. J. Hay, in *Methods of Electronic Structure Theory*, ed. H. F. Schaefer, Plenum, New York, 1977, p. 1.
11 M. Couty and M. B. Hall, *J. Comput. Chem.*, 1996, **17**, 1359.
12 T. Clark, J. Chandrasekhar, G. W. Spitznagel and P. v. R. Schleyer, *J. Comput. Chem.*, 1983, **4**, 294.
13 S. F. Boys and F. Bernardi, *Mol. Phys.*, 1970, **19**, 553.
14 (*a*) S. Sakaki and K. Ohkubo, *Inorg. Chem.*, 1989, **28**, 2583; (*b*) S. Sakaki and Y. Musashi, *Inorg. Chem.*, 1995, **34**, 1914; (*c*) S. Sakaki and Y. Musashi, *J. Chem. Soc.*, *Dalton Trans.*, 1994, 3047.
15 K. Fukui, *Acc. Chem. Res.*, 1981, **14**, 363.
16 A. E. Reed, L. A. Curtiss and F. Weinhold, *Chem. Rev.*, 1988, **88**, 899.

*Received* 25*th November* 1997; *Paper* 7/08540K